American Journal of Civil Engineering and Architecture, 2019, Vol. 7, No. 2, 52-60
Available online at http://pubs.sciepub.com/ajcea/7/2/2
Published by Science and Education Publishing
DOI:10.12691/ajcea-7-2-2

A Numerical Modelling for Seismic Behavior of Frames with CFST Composite Columns and Torsional Semi-Rigid Connection

F. Nejati[1], M. Mansoor Kiaie[1], S. A. Edalatpanah[2,*]

[1]Department of Civil Engineering, Ayandegan Institute of Higher Education, Tonekabon, Iran
[2]Department of Research Center, Ayandegan Institute of Higher Education, Tonekabon, Iran
*Corresponding author: saedalatpanah@gmail.com

Received January 03, 2019; Revised February 05, 2019; Accepted March 10, 2019

Abstract Concrete filled steel tubes (CFST) are widely used in engineering structures due to their high strength, ductility, and flexibility and also their easy construction and good economic aspect. Using the connection plates with the blind bolts in these systems can reduce the issue of weld breakage and considerably increase the seismic performance of rigid structures. This research examines and models a new semi-clamped beam to column connection using the finite element method. The main features of this connection are the use of an end plate that connects the beam to the column flange. The numerical analysis of the seismic behavior and failure modes of CFST members that have blind bolts with a semi-rigid connection (bolted with threaded rods) have been studied with the Abaqus software. This examination showed that using double bearing plates and thicker covering plate can be useful in improving the seismic performance of the connection up to 20 percent.

Keywords: *concrete filled steel tubes (CFST), ductility, flexibility, high strength, finite element method*

Cite This Article: F. Nejati, M. Mansoor Kiaie, and S. A. Edalatpanah, "A Numerical Modelling for Seismic Behavior of Frames with CFST Composite Columns and Torsional Semi-Rigid Connection." *American Journal of Civil Engineering and Architecture*, vol. 7, no. 2 (2019): 52-60. doi: 10.12691/ajcea-7-2-2.

1. Introduction

The CFST columns are used in braced structures or moment frame by using cold rolled sections. CFST columns are constructed from plates welded to each other, and the tubes are used in high rise structures having cylindrical columns. In many countries such as Japan, these columns are used in bridge piers and piers of the port breakwater. CFSTs have high strength against vibration and display good strength against one-way bending along with axial load [1,2,3,4].

This box is very suitable for high rise buildings considering their low cost of construction. Therefore, using high-strength concrete in these boxes makes them a better choice compared to reinforced concrete columns in terms of both cost and strength [5].

The response of CFST columns to the earthquake forces in the hysteresis diagram shows a considerable energy absorption by these columns. Notably, for CFST columns in which the concrete provides the main strength the stiffness reduction is observed. While this decreasing trend should be gradual and intermediate for normal materials. The main goals of this research are columns which are completely filled with concrete [1,6].

Several studies have been done to increase the strength. These investigations revealed that a reasonable connection could be created between the beam, steel box, and the concrete inside the column steel box by using long or threaded bolts [7,8].

Figure 1. Bolt

Studies also revealed that the optimal number of bolts in a column is 2 and near the column corners.

When bolted connections and filled steel tubes are used as columns, blind bolts can be used instead of normal structural bolts to avoid the need to the access to the inside of the tubes for tightening the bolt [9,10].

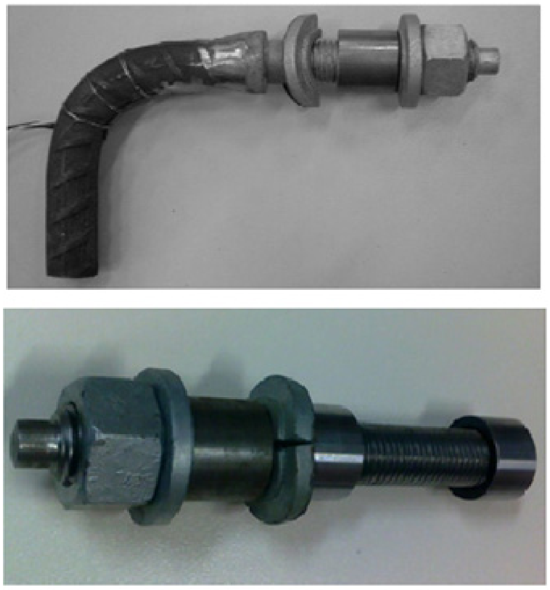

Figure 2. Two sample bolts with different heads

In order to obtain a strong and powerful connection, bolts have been previously modified by increasing its shank length inside the concrete and by putting another nut at the other end of bolt shank. Another progress here for reaching the highest possible tensile strength in these types of fastened connections is made by installing another extra head in the middle of the bolt shank moment which is called the first embedded head [11].

2. Validation

2.1. Description of an Experiment Conducted by Lee et al.

In this investigation, the seismic behavior of steel beam connection to the concrete column embedded in the steel box is evaluated. The tensile behavior of the connection under study is evaluated and validated in this test.

Totally, three T-shaped specimens were tested which are described in the following. The specimen details are illustrated in Figure 3. All the specimens were steel columns filled with concrete. The steel column section was $150\times150\times6mm$. A steel plate is connected to a steel column by four bolts which bear the tensile force.

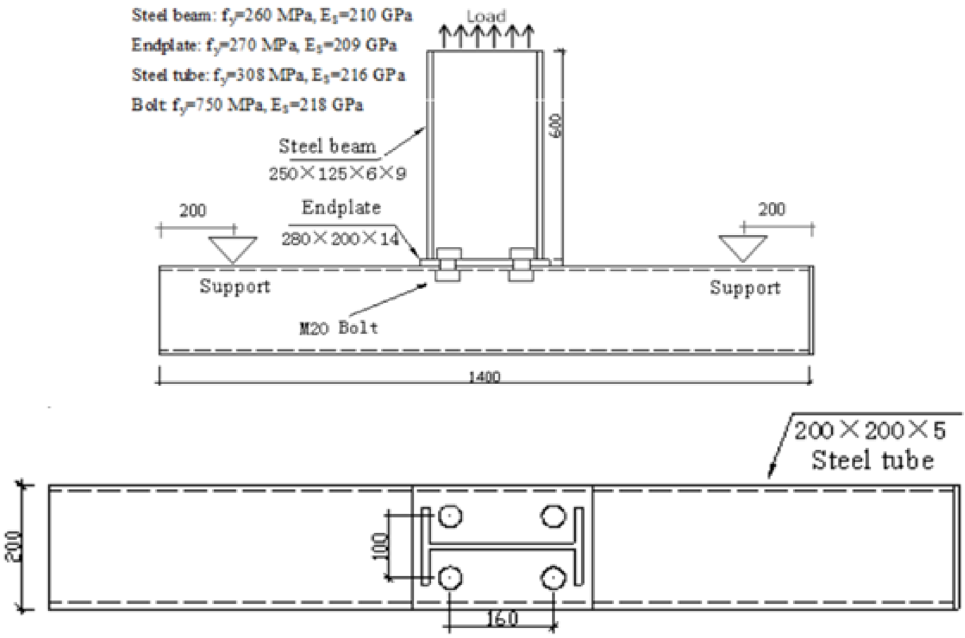

Figure 3. Specimens Description

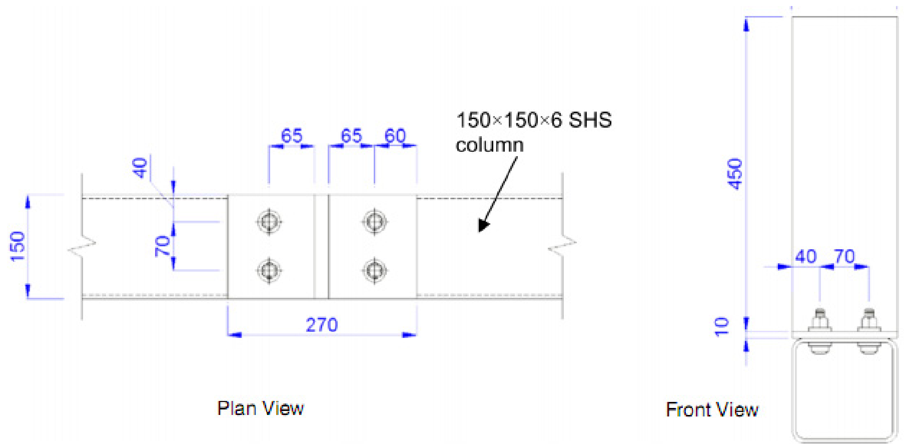

Figure 4. Location of bolts

Table 1. Specimen properties

Product Code	Bolt Size	Bolt Diameter D_1	Clamping Thickness Range (W)	Sleeve		Collar		Clamping Thickness (t_2)	Solid Cone Thickness (D_3)	Cone angle/slope
				Length (L)	Outer Diameter (D_2)	Heigh t (t_1)	Outer Diameter			
HB16-1	M16		12-29	41.5				a	L-t_2	
HB16-2	M16	16	29-50	63	27.75	8	27.75	a	L-t_2	15
HB16-3	M16		50-71	84				a	L-t_2	
HB20-1	M20		12-34	50				a	L-t_2	
HB20-2	M20	20	34-60	76	32.75	10	32.75	a	L-t_2	15
HB20-3	M20		60-68	102				a	L-t_2	

As can be seen, the column length is the distance between two supports which is equal to 1400 millimeters. The geometric dimensions and properties of the modelled bolts are presented in Table 1.

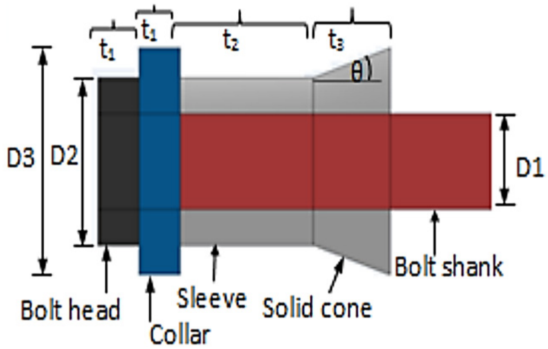

Figure 5. Parts of the bolt

The hydraulic jack above the beam imposes an axial force equal to 1000 KN during the test [12]. The steel strength properties and the concrete compressive strength are presented in the following table, respectively.

Table 2. Steel material properties

Item	Beam	Bolt
$f_y(MPa)$	500	640
$E_0(MPa)$	200000	200000

The analysis results were compared to the experimental results to evaluate the finite element model. The beam shear response diagrams are illustrated in Figure 6. The comparison between analysis results and test results reveals that they have a good agreement in shear response versus the beam end displacement during the whole loading until the failure. The initial stiffness and the ultimate strength of the modelled specimens were extremely close to those of the experimental specimens. Moreover, the uniform responses of the finite element specimens are presented in the following.

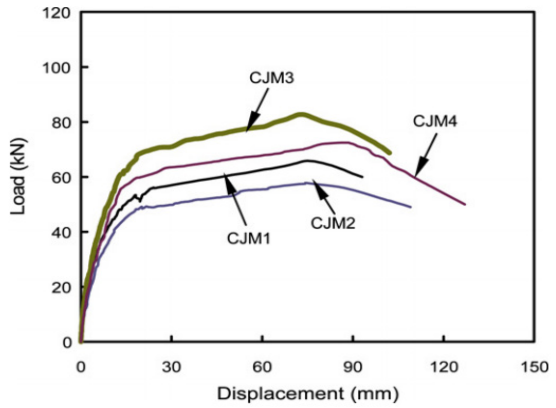

Figure 6. CJM1-4 specimen response from the experimental results

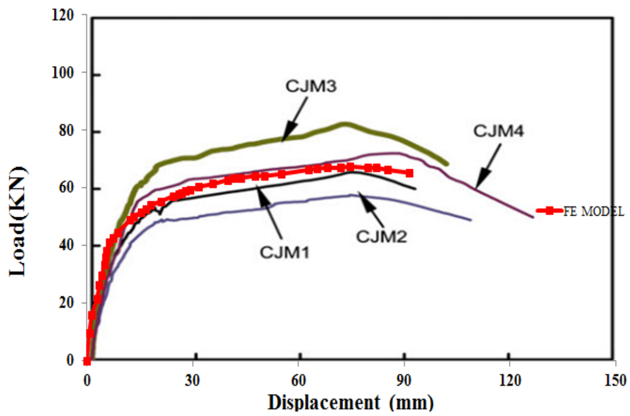

Figure 7. CJM1-4 specimen response from the finite element results compared to the experimental results

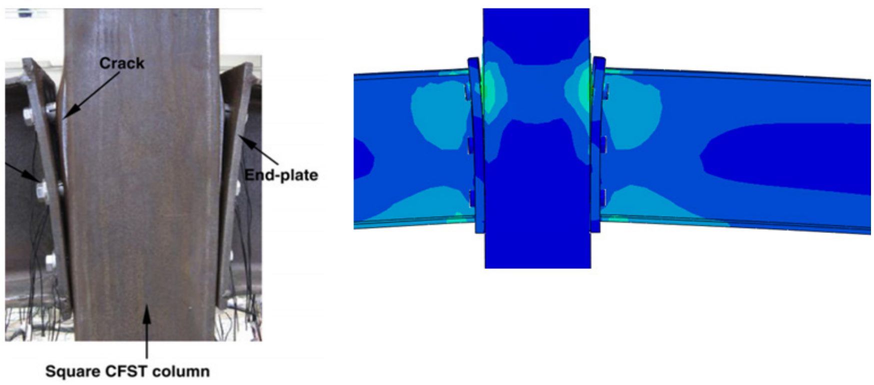

Figure 8. Specimen CJM1-4 deformed response from the finite element results compared to the experimental results

2.2. Finite Element Modelling

2.2.1. Specimen Common Parts Modelling

The model geometry for all the specimens has components such as steel column, steel beam, other steel components, and rigid supports and the loading is separately applied in the software as presented in Figure 9, and finally, by assembling these components, the whole specimen is completely constructed in the software environment. Since constraints and interactions between components have considerable effects on the analysis results they were precisely applied.

As can be seen from the above figure the bolts were modelled as rectangular after being simplified to facilitate the meshing and avoid any irregular elements in the finite element model and prevent the stress concentration.

The concrete columns are modelled by 3D elements which are, in fact, 8-node elements used for nonlinear analysis including contact between two objects, large deformation, plasticity and fracture. Steel beams and other attached components are meshed using C3D8R elements as illustrated in Figure 10. The support rigid plates are modelled as Rigid Body constraint which constrains the movements of a plate to a point like a rigid plate so the load can be applied to this reference point. The element dimensions are 20 millimeters in all sections but are considered to be 5 millimeters for bolts and connection plate (Figure 10 and Figure 11).

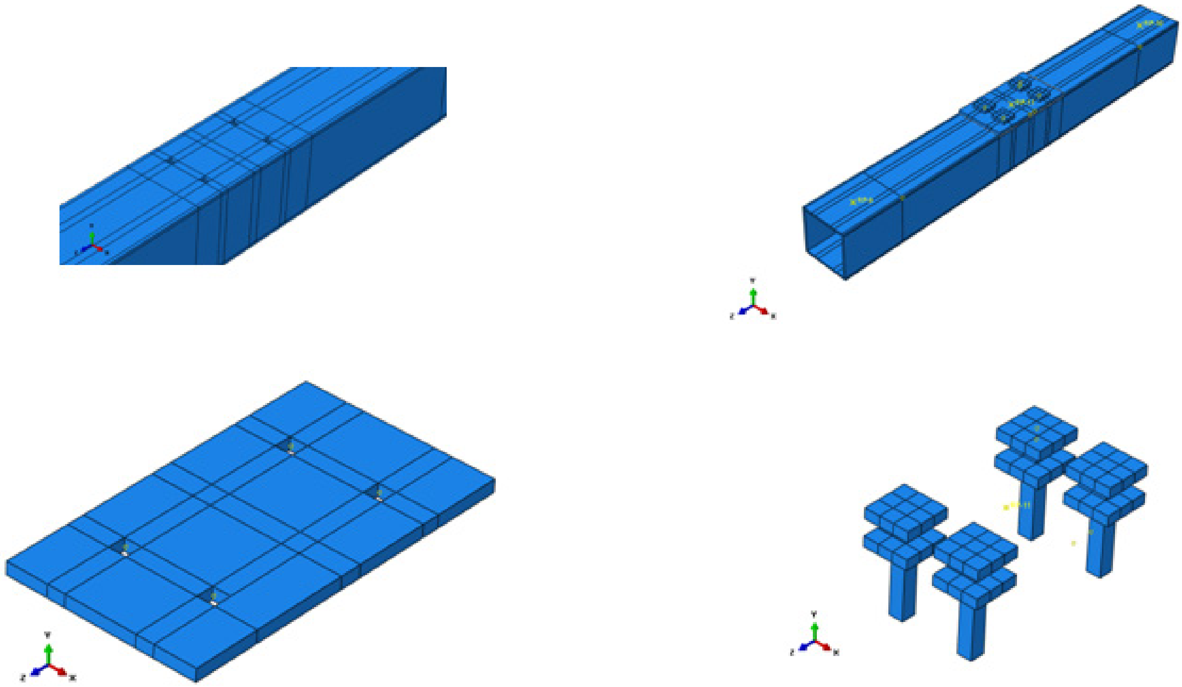

Figure 9. Different connection components in the FE model

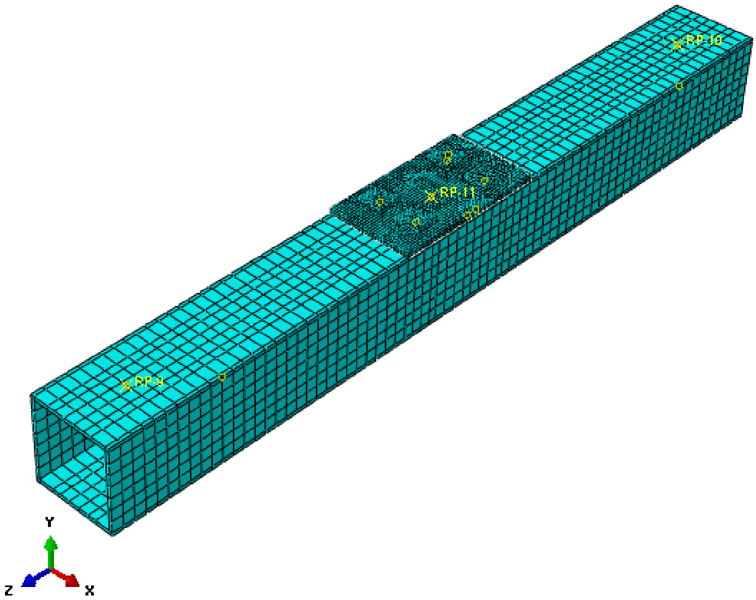

Figure 10. Elements of column, bolt and connection plate

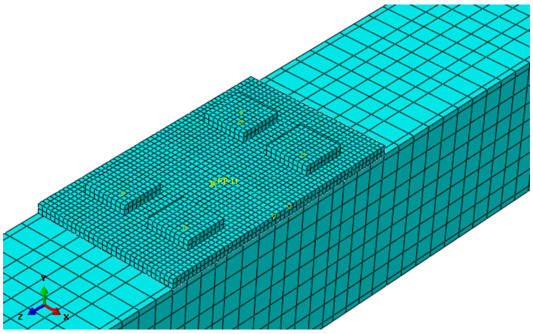

Figure 11. Close-up view of steel parts meshing

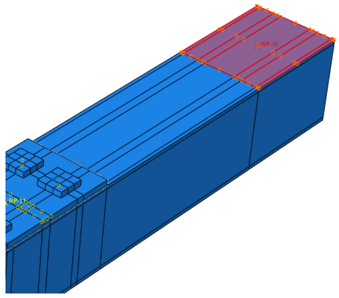

Figure 12. Defining Rigid Body constraint and the reference point in the FE model

2.2.2. Interaction and Constraint Conditions between Different Components

The Surface-to-Surface constraint was used where the steel and concrete were in contact having the friction coefficient of 0.25 which is illustrated in Figure 12. Moreover, Rigid Body constraint was used for the connection between the support plates and the column which binds all the degrees of freedom of the column plates to the rigid plates. [13,14] A reference point was also defined for the rigid plates the degrees of freedom of which are affected by this point. When a Tie constraint is defined, and two surfaces are attached one of them should be defined as the Master surface, and the other one should be defined as the Slave surface. According to the software guide, the salve surface should be the surface with softer material and smaller elements compared to those of the Master surface. Therefore, when this constraint is used, the displacements of the Slave surface points are obtained from the displacements of the Master surface points, and the relative slip between these two surfaces is neglected [15,16].

2.2.3. Boundary Condition

The two ends of the steel column in the tests are simply supported. Thus, all its translational degrees of freedom are locked in the software. This boundary condition is indeed applied to the reference point of the rigid plate which affects the movements of other nodes. In the laboratory tests, a hydraulic exciter keeps the column in its present situation before the test initiation and allows it to rotate only in the plane [17,18,19,20].

2.2.4. Finite Element Model and Element Meshing

The concrete column is modelled by 3D elements which are, in fact, 8-node elements used for nonlinear analysis including contact between two objects, large deformation, plasticity and fracture. Steel beams and other attached components are meshed using C3D8R elements as illustrated in Figure 13. Moreover, to reduce the computation time big elements were used in most areas while smaller elements were used in connection zones. The element dimensions were set to 18 mm. The bolts meshed with the dimension of 5 millimeters.

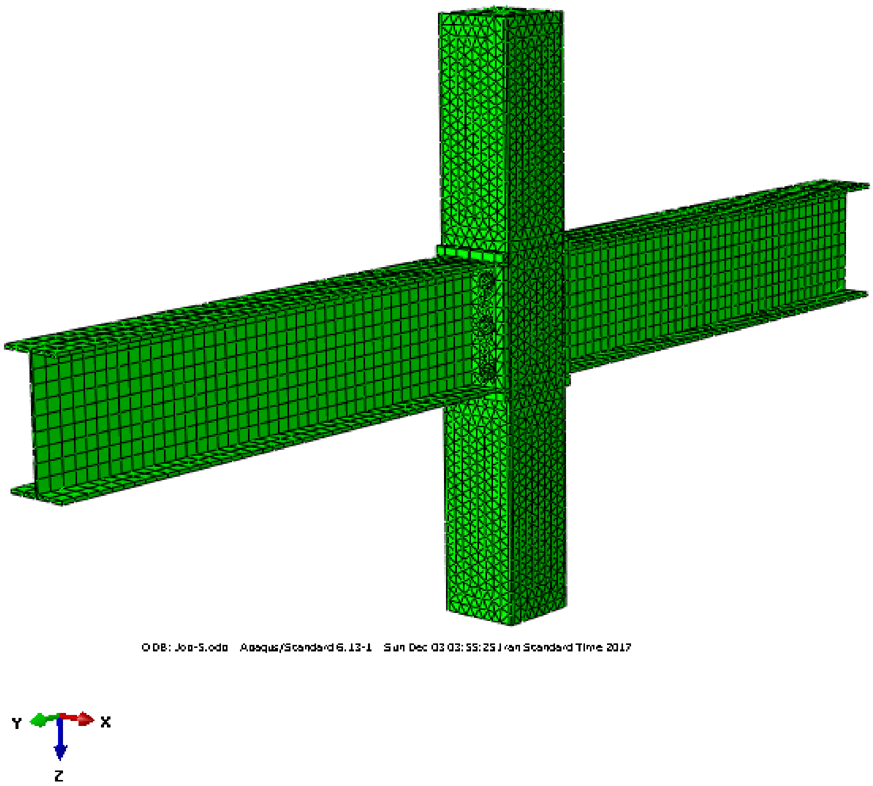

Figure 13. Finite element model meshing

The nonlinear static analysis (static general) was used to analyze the model considering the nonlinear geometric and material effects. The model analyzed in two steps wherein the first step, the gravity load was applied to the column, and in the second step, the lateral displacement applied to the tip of the column.

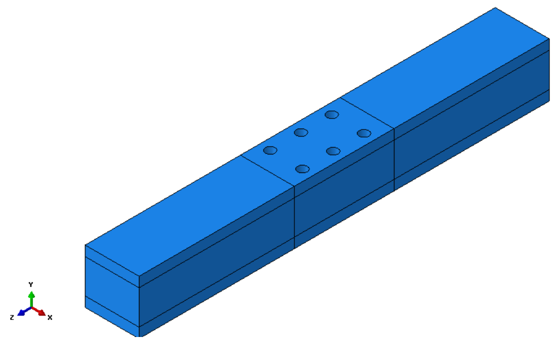

Figure 14. Bolt to concrete column connection zones embedded in the steel box

The interaction between the steel and concrete parts in the connection zone was considered by defining Tangential Behavior contact elements and the Penalty method with the friction coefficient of 0.3. The Normal Behavior contact elements with Hard Contact were defined in the connection zone to prevent the steel and concrete parts from penetrating each other. All the contact properties in the above are determined by General Contact for the software so that by defining this contact element, the software assigns the specified properties to all the concrete and steel surfaces which are in contact with each other.

2.2.5. Examining the Finite Element Analysis Results

In the beginning, the finite element specimen S1 was tested and validated to ensure that the intended specimen is correctly modelled and the assumed parameters have reasonable values and it was observed that the finite element results and the laboratory results are in good agreement with each other.

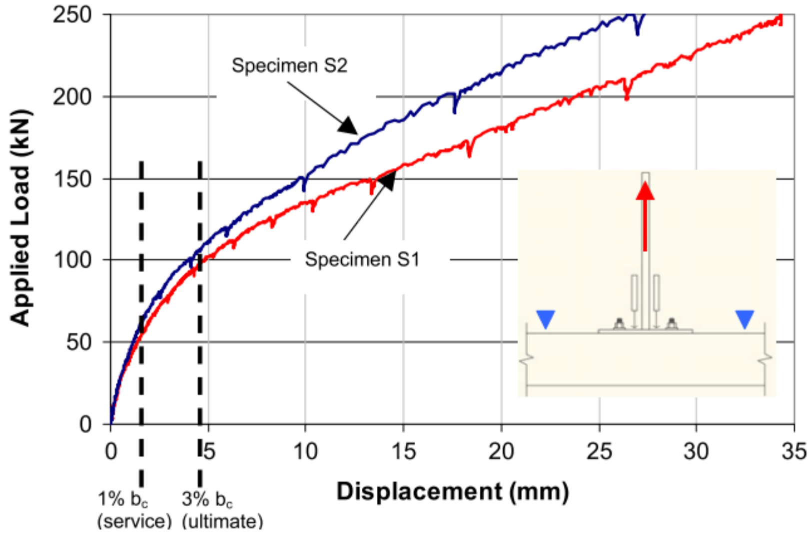

Figure 15. Force versus displacement applied to the middle of the column in the laboratory model

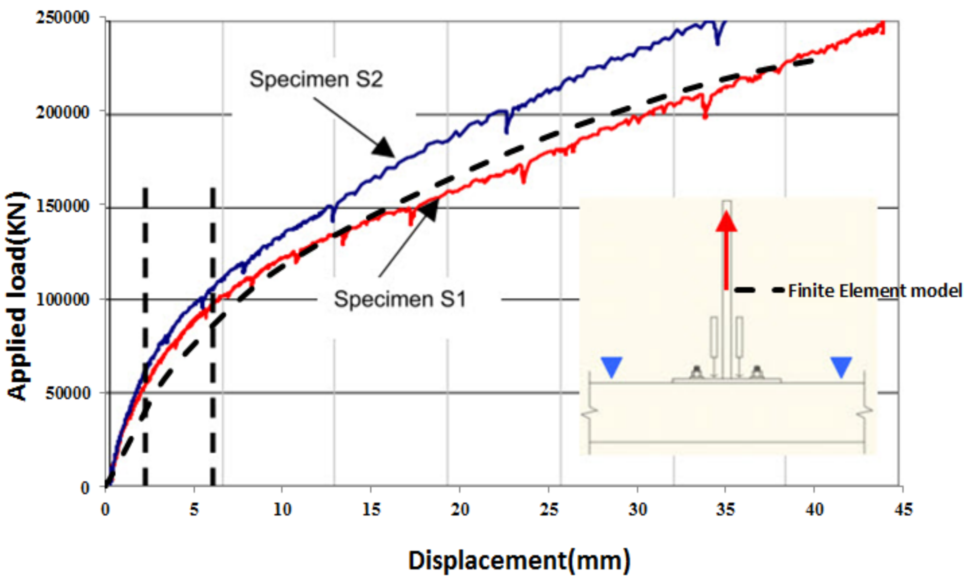

Figure 16. The comparison between the force and the displacement applied to the middle of the column in the FE and laboratory models

As can be seen from Figure 15 and Figure 16, the numerical analysis results and the laboratory results match and display similar and stable behavior.

Figure 17 shows the end of the test for specimens S1.

As (Figure 18) can be observed, the connection plate has detached from the steel column by nearly 7 millimeters in the middle, and this detachment decreases by moving away from the middle and is entirely symmetrical.

2.2.6. Stress Distribution in the Steel Plate

Almost 35 millimeters of the middle of the web steel plate reaches the yield stress in the displacement and more areas of the plate gradually achieve the yield stress by increasing the displacement. Figure 19 shows the stress distribution trend in the steel connection plate in the connection zone.

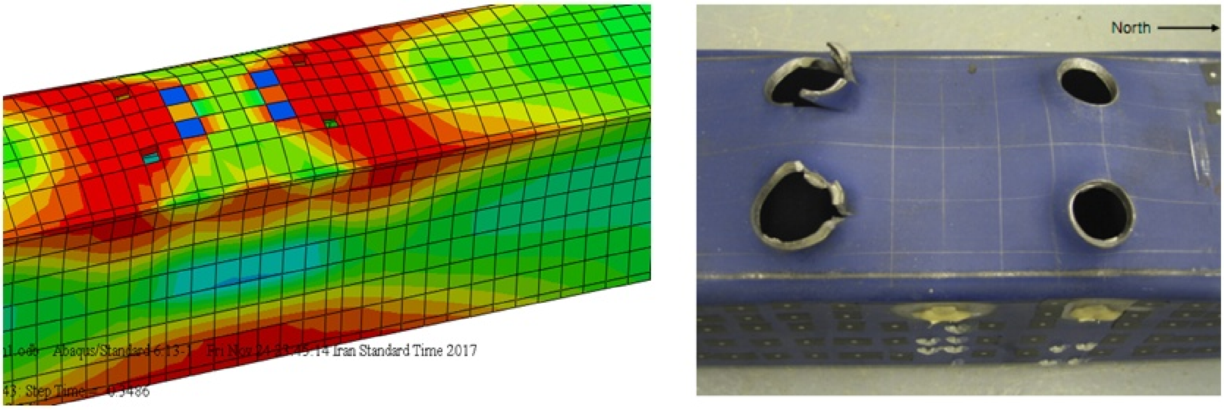

Figure 17. Deformed bolt location in the laboratory model and FE model

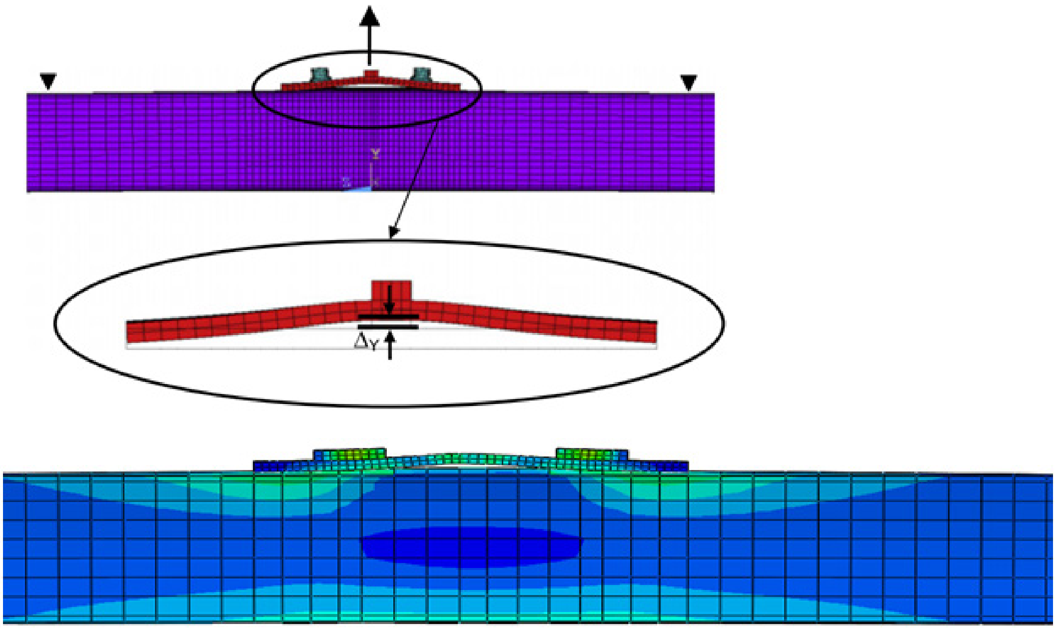

Figure 18. Deformed connection plate and the bolt location in the FE model

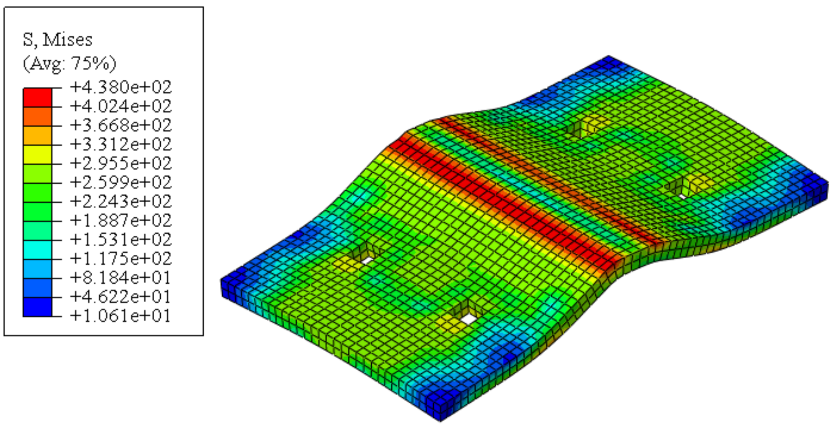

Figure 19. Stress distribution in the connection plate

2.2.7. Stress Distribution in Bolts

Almost 35 millimeters of the middle of the web steel plate reaches the yield stress in the displacement and more areas of the plate gradually achieve the yield stress by increasing the displacement. Bolts bear higher stresses which can be seen in the figure below. These stresses were maximum in those sections of bolts which were between the connection plate and the column plate.

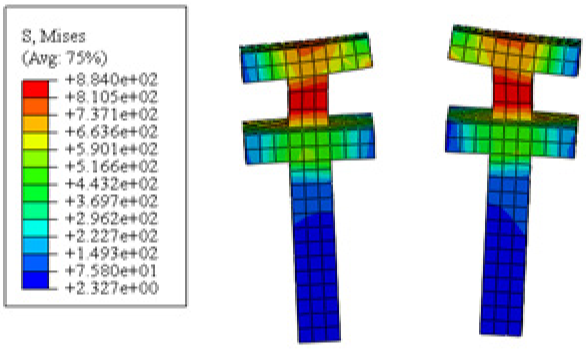

Figure 20. Stress distribution in the bolts

2.2.8. Examining the Connection Plate Thickness Effect

As can be seen from the below diagram, increasing the thickness of the connection plate can considerably increase the connection strength. Three different values were considered for the connection thickness in this study. These values are 10 millimeters, 20 millimeters and connection plate with high strength. It can be seen that the small variation in the plate thickness had no notable effect on the initial stiffness but increased the ultimate strength. But by increasing the stiffness of the connection plate by several times, the initial stiffness will also be increased.

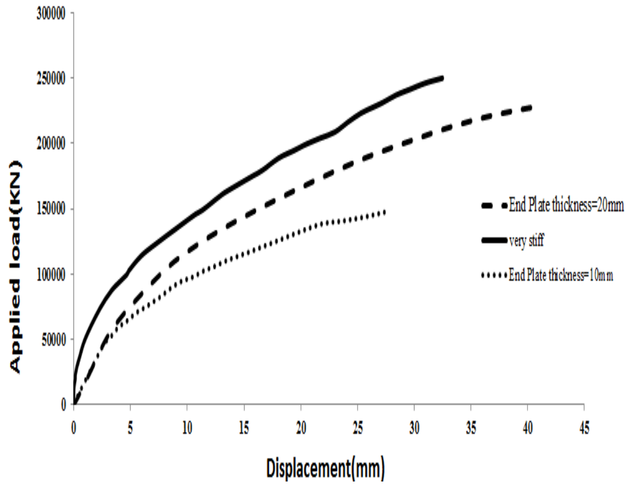

Figure 21. Force versus displacement diagram for various thicknesses of the connection plate

3. Conclusion

This study examines and models a new semi-clamped beam to column connection using the finite element method. Using an end plate which connects the beam to the column flange is of the main features of this connection. It can be observed that the plate dimensions and geometry and also the bolt configuration can have significant effects on the connection behavior. Various models with diverse dimensions and geometry were modelled and assessed in this research using the three-dimensional finite element model the results of which were compared to each other and are summarized in the following.

- By comparing the analysis and the laboratory results, it was found that the shear responses against the displacement of the beam's end are in good agreement during the whole loading until the failure. The initial stiffness and the ultimate strength of the modelled specimens were extremely close to those of the laboratory specimens.
- Almost 35 millimeters of the middle of the web steel plate reaches the yield stress in the displacement and more areas of the plate gradually achieve the yield stress by increasing the displacement. Meanwhile, bolts bear higher stresses, and these stresses were maximum in those sections of bolts which were between the connection plate and the column plate.
- As it was found, increasing the connection plate thickness considerably increases the connection strength. Three different values were considered for the connection thickness in this study. These values are 10 millimeters, 20 millimeters and a connection plate with high strength. It can be seen that the small variation in the plate thickness has no notable effect on the initial stiffness but increases the ultimate strength. But by increasing the stiffness of the connection plate by several times, the initial stiffness will also be increased.
- Based on the diagrams, one can say that increasing the plate thickness leads to an increase in the initial stiffness and the stability of the connection.

References

[1] Loh, H. Y., Uy, B., & Bradford, M. A. (2006). The effects of partial shear connection in composite flush end plate joints Part I—experimental study. Journal of Constructional Steel Research, 62(4), 378-390.

[2] Li, T. Q., Nethercot, D. A., & Choo, B. S. (1996). Behaviour of flush end-plate composite connections with unbalanced moment and variable shear/moment ratios—I. Experimental behaviour. Journal of Constructional Steel Research, 38(2), 125-164.

[3] Da Silva, L. S., Simoes, R. D., & Cruz, P. J. (2001). Experimental behaviour of end-plate beam-to-column composite joints under monotonical loading. Engineering Structures, 23(11), 1383-1409.

[4] Xiao, Y., Choo, B. S., & Nethercot, D. A. (1996). Composite connections in steel and concrete. Part 2—Moment capacity of end plate beam to column connections. Journal of Constructional Steel Research, 37(1), 63-90.

[5] Liu, Y., Málaga-Chuquitaype, C., & Elghazouli, A. Y. (2012). Response and component characterisation of semi-rigid connections to tubular columns under axial loads. Engineering structures, 41, 510-532.

[6] Mirza, O., & Uy, B. (2011). Behaviour of composite beam–column flush end-plate connections subjected to low-probability, high-consequence loading. Engineering Structures, 33(2), 647-662.

[7] Wang, J. F., Han, L. H., & Uy, B. (2009). Behaviour of flush end plate joints to concrete-filled steel tubular columns. Journal of Constructional Steel Research, 65(4), 925-939.

[8] Wang, J., Zhang, L., & Spencer Jr, B. F. (2013). Seismic response of extended end plate joints to concrete-filled steel tubular columns. Engineering Structures, 49, 876-892.

[9] Li, X., Xiao, Y., & Wu, Y. T. (2009). Seismic behavior of exterior connections with steel beams bolted to CFT columns. Journal of Constructional Steel Research, 65(7), 1438-1446.

[10] Wang, J., & Guo, S. (2012). Structural performance of blind bolted end plate joints to concrete-filled thin-walled steel tubular columns. Thin-Walled Structures, 60, 54-68.

[11] Wang, J., Chen, X., & Shen, J. (2012). Performance of CFTST column to steel beam joints with blind bolts under cyclic loading. Thin-Walled Structures, 60, 69-84.

[12] Elghazouli, A. Y., Málaga-Chuquitaype, C., Castro, J. M., & Orton, A. H. (2009). Experimental monotonic and cyclic behaviour of blind-bolted angle connections. Engineering Structures, 31(11), 2540-2553.

[13] Nakashima, M., Matsumiya, T., Suita, K., & Zhou, F. (2007). Full-scale test of composite frame under large cyclic loading. Journal of Structural Engineering, 133(2), 297-304.

[14] Han, L. H., Wang, W. D., & Tao, Z. (2011). Performance of circular CFST column to steel beam frames under lateral cyclic loading. Journal of Constructional Steel Research, 67(5), 876-890.

[15] Han, L. H., Wang, W. D., & Zhao, X. L. (2008). Behaviour of steel beam to concrete-filled SHS column frames: Finite element model and verifications. Engineering Structures, 30(6), 1647-1658.

[16] Wang, W. D., Han, L. H., & Zhao, X. L. (2009). Analytical behavior of frames with steel beams to concrete-filled steel tubular column. Journal of Constructional Steel Research, 65(3), 497-508.

[17] Wang, J., Wang, J., & Wang, H. (2017). Seismic behavior of blind bolted CFST frames with semi-rigid connections. Structures, 9, 91-104.

[18] Wang, J., & Wang, H. (2018). Cyclic experimental behavior of CFST column to steel beam frames with blind bolted connections. International Journal of Steel Structures, 18(3), 773-792.

[19] Li, B., Wang, J., Lu, Y., Zhang, Z., & Wang, J. (2019). Seismic response tests and analytical assessment of blind bolted assembly CFST frames with beam-connected SPSWs. Engineering Structures, 178, 343-360.

[20] Zhang, Z., Wang, J., Li, B., & Zhao, C. (2019). Seismic tests and numerical investigation of blind-bolted moment CFST frames infilled with thin-walled SPSWs. Thin-Walled Structures, 134, 347-362.